University of Tehran Press

Online ISSN: 2345-475X

DESERT

Home page: https://jdesert.ut.ac.ir/

Assessment of Remote Sensing Images and Products in Mapping Mangrove Forests of Iran (Northern Coasts of the Persian Gulf and the Gulf of Oman)

Mohammadreza Miandej[1], Qadir Ashournejad[1*], Fateme Garshasbi[1]

[1] Department of Geography and Urban Planning, Faculty of Humanities and Social Sciences, University of Mazandaran, Babolsar, Mazandaran, Iran E-mail: ashournejad@umz.ac.ir

Article Info.

Article type:
Research Article

Article history:
Received: 27 Sep. 2024
Received in revised from: 15 Nov. 2024
Accepted: 14 Dec. 2024
Published online: 27 Dec. 2024

Keywords:
Mangrove forests,
Remote sensing,
Mangrove Vegetation Index (MVI),
Random Forest (RF) classification.

ABSTRACT

Mangrove forests play a vital role in providing ecosystem services such as coastal protection and mitigating the impacts of climate change, necessitating mapping for assessment, monitoring, conservation, and management. Advances in remote sensing have enabled rapid and accurate mapping of these forests. This study aims to determine the best method for mapping Iran's mangrove forests (northern coasts of the Persian Gulf and the Gulf of Oman) by comparing the Mangrove Vegetation Index (MVI) and Random Forest (RF) classification using Landsat-9 and Sentinel-2 satellite data, as well as evaluating the accuracy of land cover products from the European Space Agency (ESA), the GLC_FCS30 land cover product, and the Global Mangrove Watch (GMW) product. The results show respective mangrove class accuracies of 95%, 84%, 91%, 86%, 83%, 80%, and 78% for MVI with Sentinel-2 data, MVI with Landsat-9 data, RF classification with Sentinel-2 data, RF classification with Landsat-9 data, ESA product, GLC_FCS30 product, and GMW product. The corresponding areas were 11,509 ha, 11,834.5 ha, 10,779.41 ha, 13,702.23 ha, 15,814 ha, 11,441.5 ha, and 11,117 ha, respectively. The findings indicate that Sentinel-2 data show higher potential than Landsat-9 data for mapping Iran's mangrove forests. Furthermore, the results demonstrate the higher accuracy of the generated maps compared to existing remote sensing products. These findings not only highlight the potential of modern remote sensing data for enhancing mangrove forest mapping but also pave the way for more precise and cost-effective monitoring strategies, which are crucial for conservation efforts in coastal ecosystems.

Cite this article: Miandej, M.R., Ashournejad, Q., Garshasbi, F. (2024). Assessment of Remote Sensing Images and Products in Mapping Mangrove Forests of Iran (Northern Coasts of the Persian Gulf and the Gulf of Oman). DESERT, 29 (2), DOI: 10.22059/jdesert.2024.100718

DOI: 10.22059/jdesert.2024.100718

Publisher: University of Tehran Press

1. Introduction

Mangrove forests, consisting of trees and shrubs distributed in tropical and subtropical regions between 30°N and 30°S latitudes, thrive in sheltered intertidal zones along coastlines (Sobhani & Danekar, 2023). These intertidal ecosystems offer diverse socio economic advantages and are highly productive (Bihamta Toosi *et al*., 2020; Ambarwari *et al*., 2023). They provide crucial ecological services, including carbon sequestration, water purification, and coastal protection (Sahraei *et al*., 2023), and act as natural barriers against natural disasters like storms and tsunamis. Mangroves, which grow in saline or freshwater soils and waters, are recognized as key habitats for biodiversity due to their remarkable capabilities in pollution filtration, water resource preservation, and nutrient storage (Lu *et al*., 2021). Furthermore, they offer fisheries resources and tourism opportunities, with the restoration of mangrove forests being up to five times more cost efficient than artificial infrastructure (Ibharim *et al*., 2015; Ashournejad *et al*., 2019a).

Mangrove forests, known for their ability to store carbon 3 to 5 times more effectively than tropical forests, play a vital role in enhancing water quality and mitigating the effects of climate change. Their ecosystem services have an estimated global economic value exceeding $800 billion annually, with Iran's share estimated at $164 million. However, over the past fifty years, 35% of mangrove forests have been degraded (Tran *et al*., 2022; Ashournejad, 2022). These ecosystems are highly productive and diverse, providing significant environmental, economic, and social benefits (Khan *et al*., 2024). Despite their importance, mangroves face considerable threats from human activities and the impacts of climate change (Zanvo *et al*., 2023). Deforestation, pollution, and sea level rise are major factors driving their degradation and loss (Gholami *et al*., 2019). As a result, generating accurate and regularly updated mangrove maps is essential for implementing effective conservation and management strategies. Up-to-date land cover data play a vital role for governments and organizations in the process of developing and implementing environmental and sustainable policies (Grekousis *et al*., 2015).

The accuracy of these mapping varies depending on the specific techniques used, the spatial and temporal resolution of the images, and the availability of ground truth data. Studies that use higher-resolution images and integrate multiple data sources show improved accuracy (Bihamta Toosi *et al*., 2020). Given the availability of comprehensive remote sensing data, various products have been developed, including land cover, vegetation indices, surface temperature, and humidity. These products are available in varying resolutions (Araujo-Barbosa *et al*., 2015; Wu *et al*., 2019). Among these products, land cover maps are of particular importance as understanding and monitoring them is crucial for environmental studies (Ashournejad, 2023).

Although land cover products are designed for use at global, regional, national, and local scales, the models used to develop these products are typically optimized with a broad, global approach. As a result, the performance and accuracy of these products at national and local scales have received less attention. Therefore, examining the characteristics of these products, evaluating their performance, and measuring their accuracy in specific environments is essential. Such efforts could significantly enhance the practical application of these data in natural resource management and environmental decision making (Wu *et al*., 2019).

In this regard, studies have been conducted in the past. Chaaban *et al*. (2022) assessed the accuracy of two land cover products, ESA WorldCover and ESRI, in the Tartous province of Syria. The results indicated accuracy rates of 78% and 74% for these products in the region. Bie *et al*. (2020) evaluated the accuracy of three land cover products, including GLC_FCS30, GlobeLand30, and FROM-GLC30, in northwestern China. The results showed accuracy rates of 87%, 85%, and 83%, respectively, for these products in the region. Liu *et al*. (2023) assessed the accuracy of three 30-meter resolution land cover products, namely GLC_FCS30,

GlobeLand30, and CLCD, in the city of Xinjiang, China. The results revealed accuracy rates of 88%, 83%, and 81%, respectively, for these products in the region. Xiao *et al*. (2024) evaluated the accuracy of three global mangrove cover products (GMW, GMD, and LREIS) in the Guangdong-Hong Kong Bay. The results showed accuracy rates of 63%, 76%, and 83%, respectively, for these products in the region

Over the past decades, remote sensing has become a powerful tool for monitoring land resources and addressing environmental and socio-economic challenges, with a wide range of remote sensing sources available (Garshasbi *et al*., 2025). Therefore, it is important to select the most suitable data or product for mapping mangrove forests, depending on the species and structure of the mangroves in the study area (Ashournejad *et al*., 2019a). Additionally, choosing an appropriate classification method is crucial for accurate mangrove mapping. Recent studies have increasingly employed machine learning algorithms such as RF, XGBoost, and LightGBM (Shen *et al*., 2023; Elmahdy *et al*., 2020; Valero *et al*., 2024; Rahman *et al*., 2020; Raza *et al*., 2024), demonstrating superior performance in mangrove mapping compared to traditional classification methods.

Numerous studies have utilized remote sensing and satellite data analysis for mapping and assessing these ecosystems. Zanganeh *et al*. (2017) analyzed mangrove changes in Bandar Abbas using multi-temporal Landsat images and classification algorithms (MLC, MD, SVM), with MLC showing the highest accuracy. Gupta *et al*. (2018) developed the Combined Mangrove Detection Index (CMRI) using Landsat-8 data in Bangladesh, outperforming other indices like NDVI and SAVI. Ashournejad *et al*. (2019b) studied mangrove changes in the Pars Special Economic Energy Zone with Landsat data (1986-2018), finding a peak in 2003 and decline by 2018. Toosi *et al*. (2019) compared four supervised algorithms (RF, SVM Radial, SVM Linear, and RDA) using Landsat data from Qeshm mangroves, with RF achieving the highest accuracy (93%). ErfaniFard and Lotfi Nasirabad (2022) evaluated mangrove indices with Landsat-8, finding the SMRI and MVI effective in Nayband Bay, Sirik, and Gwadar Bay. Miraki *et al*. (2023) mapped mangrove forests in Qeshm, Khamir, and Sirik using Sentinel-2 data in Google Earth Engine (GEE). The Random Forest algorithm, with MMRI and spectral indices, achieved the highest accuracy in Qeshm (98%, kappa = 0.73). Despite significant advances in the use of remote sensing for mapping mangrove forests, existing studies have primarily focused on individual datasets and have not provided a comprehensive evaluation comparing the most widely used methods and remote sensing products across the geographic distribution of mangrove forests in Iran.

Mangrove forests along the arid and semi-arid coasts of Iran exhibit unique ecological features due to their adaptation to harsh environmental conditions. This study employs remote sensing techniques to map and monitor these coastal ecosystems, providing valuable insights into understanding vegetation dynamics in dryland areas. Given the high potential of the Mangrove Vegetation Index (MVI) in distinguishing mangrove from non-mangrove cover, compared to other existing indices, it has been demonstrated in previous studies as an innovative approach for mapping these forests (Baloloy *et al*., 2020). This study also employs the Random Forest (RF) algorithm, a widely used ensemble classifier in remote sensing due to its ability to handle high-dimensional data and multicollinearity while maintaining robustness against overfitting (Belgiu & Drăguţ, 2016). Therefore, the aim of this research is to identify an effective method for mapping mangrove forests in Iran (on the northern shores of the Persian Gulf and Gulf of Oman) by comparing the MVI and

RF classification methods using Landsat-9 and Sentinel-2 satellite data. Moreover, mangrove forests in Iran are distributed sparsely, and the MVI index does not perform well

across all regions. As a result, this study addresses the identification of an appropriate threshold for using the MVI index in accurate mapping of mangrove forests in Iran. Additionally, this research seeks to evaluate the performance of land cover products (GLC_FCS30, ESA WorldCover, and Global Mangrove Watch) at the national scale, specifically in the mangrove forests of southern Iran, to assess the accuracy of these products in monitoring and managing this ecosystem. In this way, this study provides researchers with the opportunity to make better decisions when selecting methods and data for mapping mangrove forests in future studies.

2. Materials and Methods

2.1. Study Area

The mangrove forests of Iran are scattered along the northern coastlines of the Persian Gulf and the Gulf of Oman. They appear as either continuous or fragmented communities (Fig. 1). These forests are dense or semi-dense in areas such as Qeshm, Khamir Port, Sirik, and Kolghan, while they are sparse and scattered in other regions. The Iranian mangrove forests, which form along creeks, bays, and waterways, extend up to the maximum tidal influence (Safiari, 2017).

Fig 1. Map of the study area (Distribution of mangroves in Iran: 1- Mahshahr Port, 2- Nakhiloo National Park, 3- Dayyer port, 4- Nayband Bay, 5- Charak Port, 6- Qeshm Mangroves and Basaeidou, 7- Dierestan Bay(Qeshm Island) ,8- BandarAbbas, 9- Dargahan(Qeshm Island), 10- Hormoz Island, 11- Kulaghan, 12- Chakhah, Kolahi and Tiyab Inlet, 13- Sirik, 14- Gabrik and Jask Protected Area, 15- Tang Port, 16- Pozm Tiyab Bay, 17- Chabahar port, 18- Gwatar

The geographic range of their distribution is from 25°10' to 30°30' North latitude and from 49°36' to 51°05' East longitude (ErfaniFard *et al*., 2023). Temperature is the primary limiting factor for mangrove distribution. However, due to their location in the enclosed bays of the Persian Gulf and Gulf of Oman, these mangroves experience high salinity as a result of a lack of freshwater input and high evaporation rates. Despite these conditions and other geographical factors, only two species, *Avicennia marina* and *Rhizophora mucronata*, respectively, out of approximately 70 mangrove species, are present in the Persian Gulf and Gulf of Oman (Naderloo *et al*., 2024).

2.2. Methods

Fig (2) illustrates the proposed process in this study for mapping mangrove forests in Iran along the northern shores of the Persian Gulf and the Gulf of Oman. Sentinel-2 and Landsat-9 satellite images were used to map the mangrove forests in the region. The MVI and the RF classification algorithm were applied to identify and distinguish mangrove forests. Additionally, the accuracy of three global land cover products—GLC_FCS30, ESA WorldCover, and Global Mangrove Watch—was assessed in the study area.

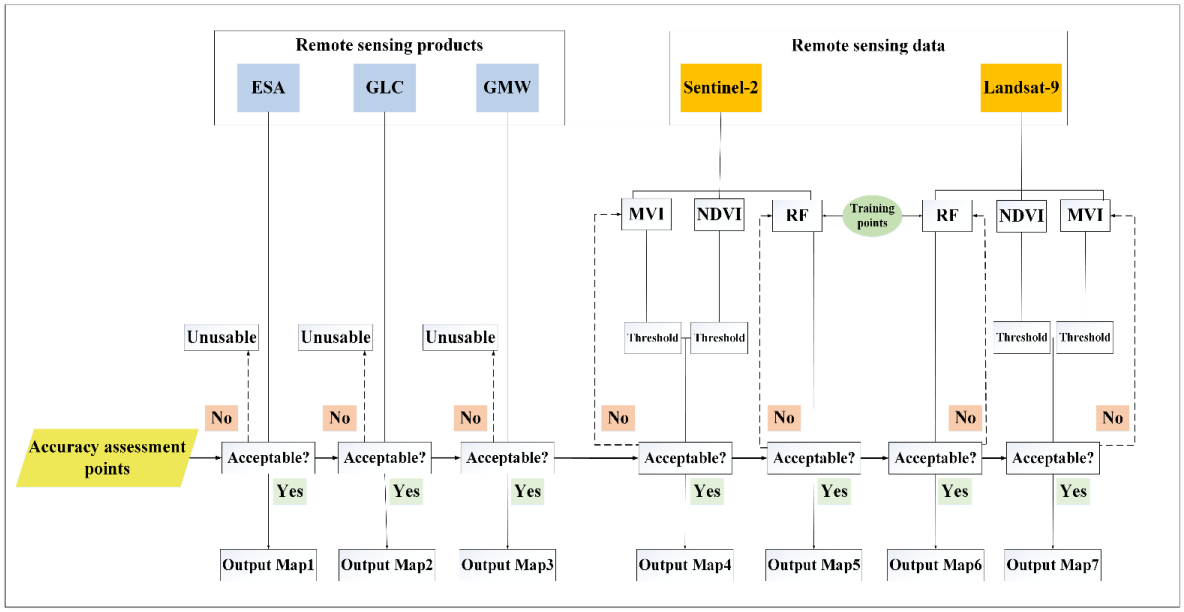

Fig 2. Conceptual model of the mangrove forest mapping process in the northern Persian Gulf and the Gulf of Oman.

2.2.1. Mangrove Forest Mapping

- MVI

To accurately map the mangrove forests along the northern shores of the Persian Gulf and the Gulf of Oman, Sentinel-2 and Landsat-9 satellite images were used. Since mangrove cover is affected by sea water during high tide, making it difficult to distinguish, selecting images from low tide periods is crucial (Erfanifard *et al*., 2022; Baloloy *et al*., 2020). Therefore, 10 satellite images from low tide conditions that covered the entire study area were selected (Table 1). These images were extracted using tide archive data from the Tides4Fishing website, and times when the sea retreat reached its maximum were identified and selected.

Table 1. Specifications of the Remote Sensing Data Used in This Study

	Landsat-9				Sentinel-2			
Image	Satellite/Sensor	Path and Row	Date	Coordinate System	Satellite/Sensor	Image ID	Date	Coordinate System
1	Landsat9/OLI	158/042	06/06/2023	WGS84/UTM/40N	Sentinel2A/MSI	T40RDQ	06/02/2023	WGS84/UTM/40N
2	Landsat9/OLI	159/042	06/13/2023	WGS84/UTM/40N	Sentinel2A/MSI	T40RGP	07/01/2023	WGS84/UTM/40N
3	Landsat9/OLI	159/041	06/13/2023	WGS84/UTM/40N	Sentinel2A/MSI	T39RWL	07/03/2023	WGS84/UTM/39N
4	Landsat9/OLI	165/039	06/23/2023	WGS84/UTM/39N	Sentinel2A/MSI	T40RHP	07/06/2023	WGS84/UTM/40N
5	Landsat9/OLI	162/042	07/04/2023	WGS84/UTM/39N	Sentinel2A/MSI	T40RBQ	07/10/2023	WGS84/UTM/40N
6	Landsat9/OLI	160/041	07/06/2023	WGS84/UTM/40N	Sentinel2A/MSI	T40RCQ	07/12/2023	WGS84/UTM/40N
7	Landsat9/OLI	156/043	07/10/2023	WGS84/UTM/41N	Sentinel2A/MSI	T39RWL	07/13/2023	WGS84/UTM/39N
8	Landsat9/OLI	163/041	07/11/2023	WGS84/UTM/39N	Sentinel2A/MSI	T41RLH	07/13/2023	WGS84/UTM/41N
9	Landsat9/OLI	161/041	07/13/2023	WGS84/UTM/40N	Sentinel2A/MSI	T40RDQ	07/27/2023	WGS84/UTM/40N
10	Landsat9/OLI	157/042	08/02/2023	WGS84/UTM/41N	Sentinel2A/MSI	T40REP	08/13/2023	WGS84/UTM/40N

In MVI, three key spectral bands are used: Near-Infrared (NIR), Short-Wave Infrared 1 (SWIR1), and Green bands (Eq 1). In Sentinel-2 satellite imagery, these bands correspond to bands 8, 11, and 3, respectively, while in Landsat-9 imagery, bands 5, 6, and 3 are used to calculate this index. The SWIR1 band is particularly crucial due to its ability to detect water absorption by vegetation, playing a key role in delineating mangrove forest boundaries (Erfanifard *et al*, 2022). Additionally, the NIR band serves as a key indicator of plant greenness and structural characteristics of vegetation. Reflectance from mangrove forests in the visible spectrum, particularly in the blue and red bands, is lower due to the strong absorption of light by chlorophyll during photosynthesis. These features, combined with the high reflectance of mangroves in the NIR and SWIR1 bands, provide ideal conditions for designing the MVI index. The combination of these three bands (SWIR1, NIR, and Green) makes the MVI index an efficient and reliable tool for accurately identifying and analyzing mangrove forest cover (Baloloy *et al*., 2020). Given that bands 3 and 8 in Sentinel-2 have a spatial resolution of 10 meters, band 11, which has a spatial resolution of 20 meters, was resampled to 10 meters. To improve the accuracy of mangrove forest identification, the Normalized Difference Vegetation Index (NDVI) was used as a complementary index to the MVI (Eq 2). NDVI, which ranges from -1 to +1, distinguishes vegetation from other land cover types, with negative values indicating areas without vegetation (Li *et al*., 2014). Therefore, to remove non-mangrove pixels from the initial MVI results that could reduce mapping accuracy, a binary image multiplication approach (MVI × NDVI) was applied. This process, a common image computation technique, allows the separation of specific areas by multiplying two binary images (0 and 1) (Fatemi & Rezaei, 2023). An appropriate threshold for NDVI was determined to retain only vegetation, while other non-vegetated surfaces and features were masked. This combined approach enhanced the accuracy of mangrove forest identification and reduced the impact of errors related to non-relevant cover types in the final mapping. Accurate mangrove forest detection relies on determining an appropriate threshold for the MVI. Although the standard threshold value is generally considered to be above 4.5 (Baloloy *et al*., 2020), it may vary depending on the structural characteristics and environmental conditions of the mangroves. In areas with lower tree density, canopy height, and greenness, lowering the threshold value can improve the accuracy of distinguishing mangroves from non-mangrove cover. This is particularly relevant for mangrove forests in the Persian Gulf and the Gulf of Oman, as these ecosystems have a weaker structure compared to riverine mangroves due to their location in coastal zones,

exposure to tidal fluctuations, and limited access to freshwater (Naderloo *et al*., 2024). Taking these factors into account, in this study, the MVI threshold was assessed and adjusted across all mangrove sites in Iran using Sentinel-2 and Landsat-9 satellite images. This process was carried out within the GEE platform, which facilitated cloud processing and analysis of extensive remote sensing data, enabling the evaluation and optimization of various threshold values. The threshold adjustment was performed experimentally by applying different values to determine the optimal threshold that ensures the highest accuracy in mangrove forest delineation.

$$MVI = \frac{NIR-Green}{SWIR1-Green} \quad (1)$$

$$NDVI = \frac{NIR-Red}{NIR+Red} \quad (2)$$

- Classification with RF

The classification of mangrove forests in this study was performed using the RF algorithm within the GEE platform. For this purpose, Sentinel-2 and Landsat-9 images (Table 1), covering the entire extent of Iran's mangrove forests, were utilized. For the classification of Landsat-9 images, the bands SR_B2, SR_B3, SR_B4, SR_B5, and SR_B6 were used, which are corrected data representing the actual surface reflectance. For Sentinel-2, the bands B1, B2, B3, B4, B5, B6, B7, B8, B8A, and B11 were used to extract the spectral characteristics of mangrove forests and other land covers. Since Sentinel-2 images include bands with varying spatial resolutions (10, 20, and 60 meters), all bands were resampled to a uniform 10-meter resolution to enhance model accuracy. This resampling was performed using the bilinear resampling method, where the value of each new pixel is calculated as a weighted average of the values of the four neighboring pixels in the original image (Lillesand *et al*., 2015). For model training, a set of 4,520 training points from three distinct classes (water, soil, and mangrove) was extracted from available data (Fatemi & Rezaei, 2023), including Google Earth images. The use of high-resolution Google Earth imagery is a common approach for assessing the accuracy of satellite image classification (Kiyani *et al*., 2014). A simple random sampling method was used to select these points to maintain class balance and ensure proper model training. All classes were defined and labeled using these 4520 training points. For the selection of the number of trees (30 trees), this value was determined empirically to strike an optimal balance between model accuracy and overfitting prevention. Initial evaluations showed that increasing the number of trees beyond 30 did not significantly improve accuracy, while reducing the number of trees decreased model accuracy and increased sensitivity to the training data. Therefore, 30 trees were selected as the optimal number for this study**.** Additionally, random feature selection for each split and a minimum sample size of 1 for node splitting were applied with the default settings of GEE. The majority voting rule was then used to determine the final class for each pixel. Given the satisfactory performance of these settings with the study data, more complex configurations were deemed unnecessary. All information regarding the default settings and the Random Forest algorithm was obtained from the GEE documentation.

2.2.2. Remote Sensing Products

Global land cover products are designed for use at various scales; however, their accuracy at local scales may not be reliable. Therefore, in this study, the accuracy of three products—GLC_FCS30, ESA WorldCover, and Global Mangrove Watch—was evaluated in the mangrove forests of southern Iran to provide researchers with insights into their regional accuracy for monitoring these ecosystems.

- ESA Land Cover Product

The ESA Land Cover product, provided by the European Space Agency, has a spatial resolution of 10 meters. This product was generated using imagery from the Sentinel-1 and Sentinel-2 satellites and the Decision Tree (DT) classification algorithm. The accuracy of the product is 75% for 2020 and 76.7% for 2021. The product consists of 11 classes based on the Land Cover Classification System (LCCS), one of which is mangrove forests (Zanaga *et al*., 2021).

- GLC_FCS30 land cover product

The GLC_FCS30 land cover product represents a significant advancement in global land cover monitoring, providing a comprehensive understanding of land cover dynamics with 30-meter resolution for the period from 1985 to 2022. Developed through continuous change detection methods and utilizing an extensive archive of Landsat images within the GEE platform, this dataset includes 35 distinct land cover types, including mangrove forests. The accuracy of this product, verified with over 84,000 global samples, is 80.88% for the base classification system (10 major land cover types) and 73.248% for the Level-1 assessment system, which includes 17 land cover types according to the Land Cover Classification System (LCCS) (Zhang *et al*., 2024).

- Global Mangrove Watch (GMW) product

The GMW program was launched in 2011. It provides spatial information on changes and the extent of mangrove forests. The program has produced global baseline maps of mangrove extent for 2010 using ALOS PALSAR and Landsat data, while tracking changes from 1996 to 2020 using JERS-1 SAR, ALOS PALSAR, and ALOS-2 PALSAR-2 data. Additionally, annual maps are available from 2018 onward. The product classifies mangrove forests using Random Forest and Artificial Neural Networks, achieving an overall accuracy of 87% (Bunting *et al*., 2022).

2.2.3. Accuracy Assessment

In this study, the accuracy of the mangrove class in maps derived from the MVI, RF classification, and remote sensing products was evaluated using 3,950 ground truth points collected through random sampling (Tso & Mather., 2003) and Google Earth imagery. Accuracy assessment was conducted using the Confusion Matrix, a common method for comparing classified data with reference data and determining their level of agreement (Congalton, 1991). This method is one of the most widely used approaches in satellite image classification accuracy assessments and enables the evaluation of the correctness of pixels classified as mangroves. In other words, this assessment determines what percentage of the pixels identified by the model as mangroves actually belong to the real mangrove cover.

3. Results

- Threshold accuracy results of MVI with Landsat-9 and Sentinel-2 images.

In this section, the results of comparing Sentinel-2 and Landsat-9 data using the MVI index for detecting mangrove forests along the northern coasts of the Persian Gulf and the Gulf of Oman are presented. Based on the MVI threshold analysis, the results indicated that Sentinel-2 data generally outperformed Landsat-9 data in detecting mangrove forests in these areas. For example, at the Qeshm site, which is one of the largest mangrove areas in the region, Sentinel-2 achieved a mangrove class accuracy of 98%, while Landsat-9 data showed a mangrove class accuracy of 88%. The estimated mangrove area at this site was 7,579.8 hectares using Sentinel-2 and 8,054.4 hectares using Landsat-9. This difference can be attributed to Sentinel-2's ability to better identify smaller and more scattered areas in addition to larger ones. At the Sirik site, Sentinel-2 also performed better than Landsat-9. Sentinel-2 data achieved a mangrove class

accuracy of 96%, while Landsat-9 data showed a mangrove class accuracy of 92%. The mangrove area at this site was estimated at 715.8 hectares using Sentinel-2 and 808 hectares using Landsat-9. For medium and smaller sites, Sentinel-2 data consistently demonstrated better performance. At the Chakhah, Kolahi, and Tiyab Inlet sites, Sentinel-2 achieved a mangrove class accuracy of 97%, compared with Landsat-9's mangrove class accuracy of 83%. The mangrove area at this site was estimated at 490.3 hectares using Sentinel-2 and 452 hectares using Landsat-9. At the Charak Port site, one of the smallest study areas, Sentinel-2 achieved a mangrove class accuracy of 89%, compared to 73% for Landsat-9. The estimated mangrove area was 6.3 hectares using Sentinel-2 and only 2.9 hectares using Landsat-9. Table 2 provides detailed mangrove class accuracy and area estimates for mangrove sites in Iran.

- Mangrove class accuracy results in the classification of Sentinel-2 and Landsat-9 images using the RF.

In this section, the results of the comparison between Sentinel-2 and Landsat-9 data using the RF algorithm for mangrove forest classification along the northern coasts of the Persian Gulf and the Gulf of Oman are presented. In the classification results, Sentinel-2 generally showed higher accuracy, but the performance of Landsat-9 was closely comparable, with Landsat-9 even showing better accuracy in some cases. For the Gabrik and Jask Protected Area, one of the largest study sites, differences between the two datasets were observed. Sentinel-2 data achieved a mangrove class accuracy of 95% and estimated the mangrove area at 924.9 hectares. In contrast, Landsat-9 data showed a mangrove class accuracy of 91% and estimated the mangrove area at 1,127 hectares. The Qeshm site also demonstrated Sentinel-2's superior performance, with a mangrove class accuracy of 96% and an estimated area of 6,154.45 hectares. In comparison, Landsat-9 data showed a mangrove class accuracy of 88% and estimated the area at 7,513.4 hectares. The Sirik site further highlighted Sentinel-2's superior performance. Sentinel-2 achieved a mangrove class accuracy of 98% and estimated the mangrove area at 783.4 hectares. In comparison, Landsat-9 data showed a mangrove class accuracy of 93% and estimated the area at 845.1 hectares. At the Chakhah, Kolahi, and Tiyab Inlet sites, Sentinel-2 achieved a mangrove class accuracy of 87% and estimated the area at 663.6 hectares. Landsat-9 data showed a slightly higher mangrove class accuracy of 90% and estimated the area at 1,060.7 hectares. For other sites, including Mahshahr Port, Kulaghan, Gwatar, and Nayband Bay, Sentinel-2 data generally showed higher mangrove class accuracy, with estimated areas typically smaller than those calculated using Landsat-9. Detailed results for all sites are presented in Table 2.

- Remote Sensing Products

Mangrove forest classifications in various regions using the ESA, GLC, and GMW products have yielded different results (Table 3). The ESA product failed to identify mangrove forests at several sites. In key sites such as Mahshahr Port, Tang Port, Chabahar Port, and Charak Port, no mangroves were detected, with mangrove class accuracy being zero. However, in regions such as Qeshm (mangrove class accuracy 93%, area 8670 ha), Kulaghan (mangrove class accuracy 90%, area 716 ha), and Sirik (mangrove class accuracy 91%, area 844 ha), acceptable performance was achieved. The GLC product performed better than ESA in many regions. It exhibited higher mangrove class accuracy at sites such as Qeshm (mangrove class accuracy 94%, area 11862 ha), Kulaghan (mangrove class accuracy 92%, area 784 ha), and Sirik (mangrove class accuracy 90%, area 919 ha). It also detected a limited area of mangroves at sites such as Tang Port (mangrove class accuracy 59%, area 2.9 ha) and Hormoz Island

Table 2. Accuracy assessment and area of mangrove sites on the northern coast of the Persian Gulf.

		Site Name	Mahshahr Port	Tang Port	Chabahar Port	Charak Port	Dayyer port	BandarAbbas	Nakhiloo National Park	Hormoz Island	Pozm Tiyab Bay	Deirstan Bay	Nayband Bay	Chakhah, Kolahi and Tiyab Inlet	Dargahan	Sirik	Qeshm	Kulaghan	Gwatar	Gabrik and Jask Protected Area
MVI	Sentinel-2	Threshold	1	1.9	1	1.2	1.5	1	1	1	1.1	1.1	1.7	1.4	1.1	1.1	1.5	1.5	1.5	1.7
		Mangrove class accuracy	95%	90%	95%	89%	87%	95%	90%	90%	95%	95%	93%	97%	98%	96%	98%	96%	96%	96%
		Area (ha)	242	5.1	32	6.3	8.8	90	14	14.6	38.2	24.3	266	490.3	118.6	715.8	7579.8	608.7	557	697
	Landsat-9	Threshold	1	2	2	2	1.7	1.5	1.5	1	1.5	1.6	1.6	2	2	1.5	1.5	1	1.5	1
		Mangrove class accuracy	83%	83%	84%	73%	75%	92%	83%	84%	75%	79%	80%	83%	98%	92%	88%	83%	83%	81%
		Area (ha)	127	3.6	41.49	2.9	3.6	131.31	9	15.1	11.3	26.8	232.2	452	182	808	8054.4	741	406	576
RF	Sentinel-2	Mangrove class accuracy	93%	92%	94%	91%	79%	85%	90%	87%	88%	77%	89%	87%	95%	98%	96%	90%	93%	95%
		Area (ha)	587	9.6	71.7	8.8	8.6	113.2	14.4	15.3	39.7	30.36	233	663.6	123.5	783.4	61.54	568.5	516.4	924.9
	Landsat-9	Mangrove class accuracy	78%	88%	93%	82%	66%	93%	68%	70%	85%	79%	83%	90%	96%	93%	88%	91%	87%	91%
		Area (ha)	736	14.5	165.2	11.4	18.68	99	24.7	22.5	111.4	40.6	272.7	1060.7	317.1	845.1	7513.4	699.7	622.6	1127
Remote sensing products	ESA	Mangrove class accuracy	0	0	0	0	0	80%	0	0	0	61%	0	84%	0	91%	93%	90%	79%	88%
		Area (ha)	0	0	0	0	0	79	0	0	0	5.6		591.4	0	844	8670	716	453	825.5
	GLC	Mangrove class accuracy	0	59%	49%	0	0	72%	0	56%	0	73%	0	84%	85%	90%	94%	92%	84%	83%
		Area (ha)	0	2.9	11.2	0	0	57	0	10.4	0	20.7	0	560	142	919	11862	784	545	910
	GMW	Mangrove class accuracy	0	0	0	0	0	79%	0	0	0	57%	0	77%	0	86%	82%	89%	71%	88%
		Area (ha)	0	0	0	0	0	87	0	0	0	7	0	580.5	0	91.2	6044.4	855	302	635.5

(mangrove class accuracy 56%, area 10.4 ha). However, it still performed poorly in areas such as Mahshahr Port, Charak Port, and Nakhiloo National Park. The GMW product showed good performance in many regions and, in some cases, produced results similar to the GLC. For example, in Qeshm (mangrove class accuracy 82%, area 6044.4 ha), Kulaghan (mangrove class accuracy 89%, area 855 ha), and Sirik (mangrove class accuracy 86%, area 91.2 ha), it demonstrated high ability in detecting mangrove forests. However, like the others, it failed to detect mangroves in areas such as Mahshahr Port, Tang Port, Chabahar Port, and Nakhiloo National Park, with mangrove class accuracy being zero, indicating an inability to detect mangroves in these regions. Fig 3 show the mangrove class for several mangrove forest sites in Iran based on the MVI threshold, the generated classifications, and remote sensing products.

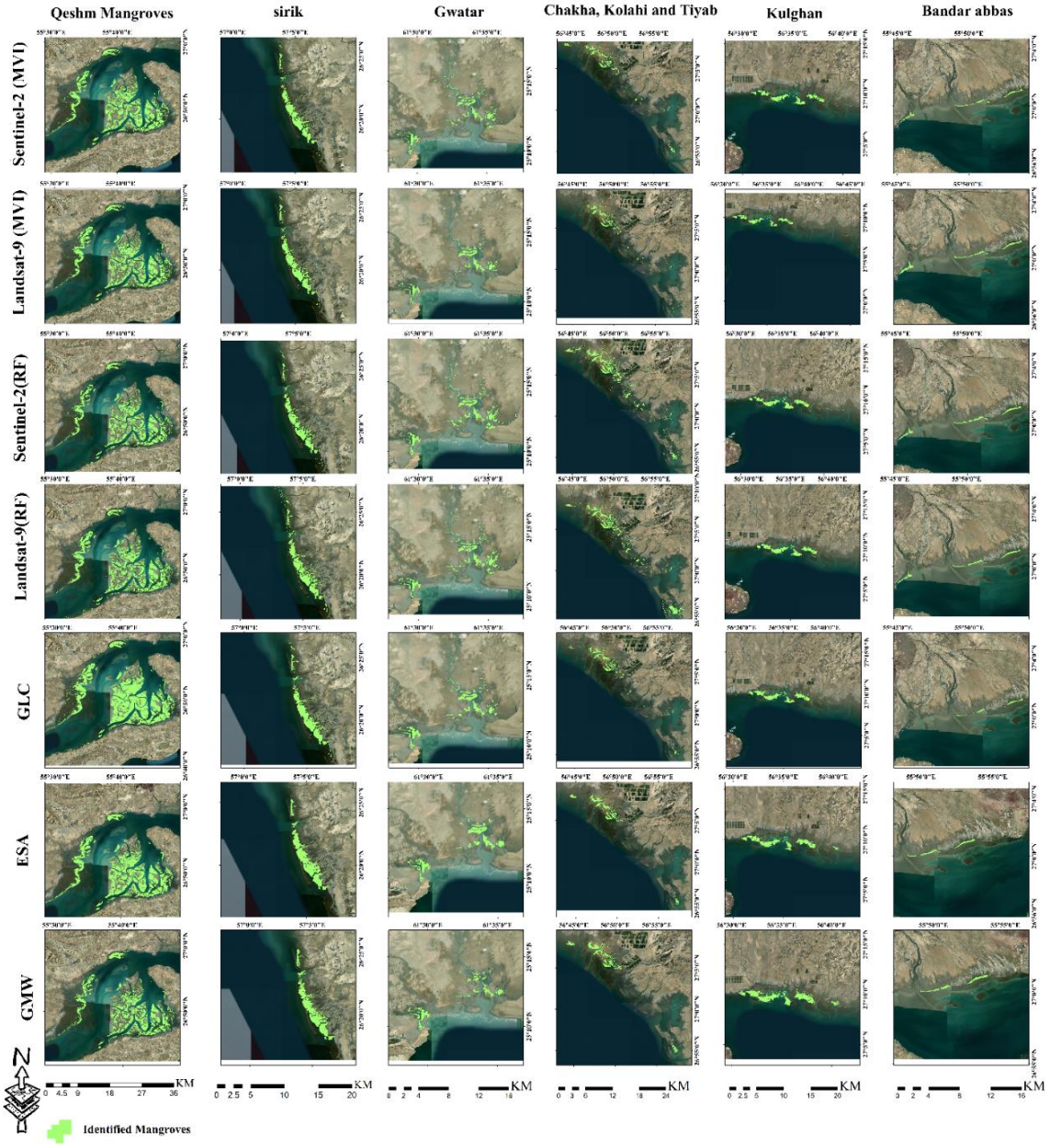

Fig 3. Geographic distribution maps of mangrove forests in Qeshm, Sirik, Gwatar, Chakhah, Kolahi and Tiyab Inlet, Kulgan, and Bandar Abbas.

The mangrove class accuracy and estimated area of mangrove forests using the MVI index,

RF classification, and global products were also calculated collectively for all studied sites, in contrast to previous analyses that evaluated accuracy separately for each of the 18 sites (Table 3). The classification based on the MVI index using Sentinel-2 showed the highest mangrove class accuracy (95%) and estimated an area of 11,509 hectares, while Landsat-9, with an accuracy of 84%, estimated a larger area of 11,834.5 hectares. The classification using the RF algorithm showed different performance, with Sentinel-2 achieving a mangrove class accuracy of 91% and estimating an area of 10,779.41 hectares, whereas Landsat-9, with an accuracy of 86%, estimated a larger area of 13,702.23 hectares. Among the global products, GLC had an accuracy of 80% and estimated the largest mangrove area at 15,814 hectares. The ESA product showed an accuracy of 83%, with an estimated mangrove area of 11,441.5 hectares, while GMW had the lowest accuracy (78%) and estimated an area of 8,605 hectares (Fig 4).

Table 3. Mangrove class accuracy and area for different methods (RF, MVI) and remote sensing products.

Maps	Mangrove class accuracy	Area(ha)
MVI (Sentinel-2)	95%	11509
MVI (Landsat-9)	84%	11834.5
RF (Sentinel-2)	91%	10779.41
RF (Landsat-9)	86%	13702.23
GLC	80%	15814
ESA	83%	11441.5
GMW	78%	8605

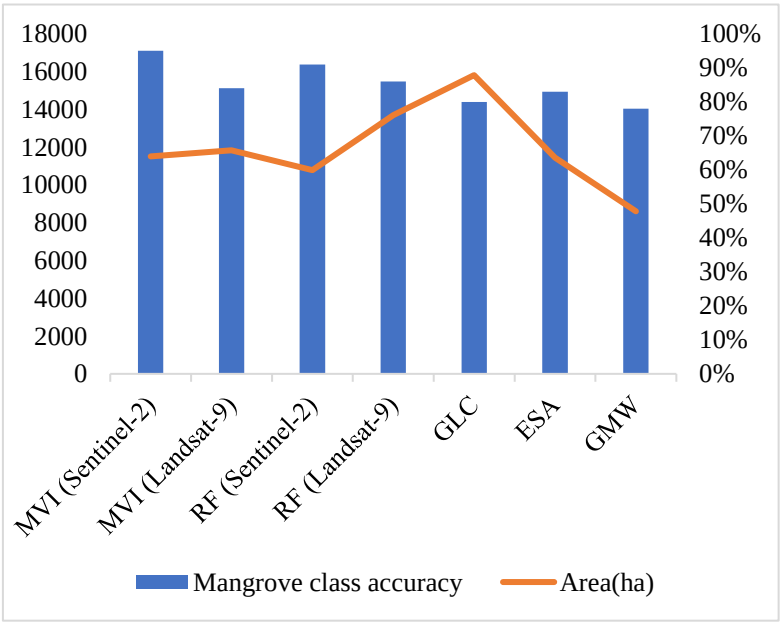

Fig 4. Comparison of mangrove class accuracy and area for different methods (RF, MVI) and remote sensing products.

4. Discussion

Unlike previous research (Zanganeh *et al*., 2017; Conopio *et al*., 2021; Neri *et al*., 2021; Yang *et al*., 2022; Jia *et al*., 2023), which mainly relied on isolated datasets, this study provides a comprehensive evaluation of remote sensing techniques, including the MVI and RF classification methods, utilizing Landsat-9 and Sentinel-2 satellite imagery. One of the primary challenges in mangrove forest mapping in Iran is the uneven distribution of mangrove areas, which complicates the performance of indices like the MVI across different regions. As a result, this study focuses on identifying an appropriate threshold for the MVI to improve its effectiveness for mapping mangrove forests in Iran. The research also highlights the performance of global land cover products, such as GLC_FCS30, ESA WorldCover, and Global Mangrove Watch, in the context of Iran's mangrove ecosystems. By evaluating their accuracy in local conditions, this study aims to enhance the practical application of these products.

The analysis of the results for determining the MVI threshold in different regions revealed that the sensitivity of the MVI threshold significantly impacts the accuracy of mangrove detection. A comparison between Sentinel-2 and Landsat-9 data showed that Sentinel-2 outperformed Landsat-9 in terms of mangrove class accuracy (98%) and higher accuracy values. Specifically, the Chakhah, Kolahi and Tiyab Inlet, Dargahan, and Qeshm regions achieved high mangrove class accuracy (98%) using Sentinel-2, demonstrating its ability to accurately identify mangroves, even in complex areas. These results are consistent with the findings of Wang *et al*. (2018) and Baloloy *et al*. (2020). On the other hand, Landsat-9 data, particularly in areas like Mahshahr Port and Tang Port, showed lower mangrove class accuracy (83%) and lower performance. Moreover, the sensitivity of the threshold in Landsat-9 data was higher. For instance, changes in the threshold in Tang Port and Chabahar significantly affected the mangrove class accuracy, highlighting the need for finer parameter adjustment for this sensor. Ultimately, the threshold analysis indicates that the accuracy of mangrove detection and the calculated area is highly dependent on the selection of an appropriate threshold and the characteristics of the sensor used.

The results of mangrove forest classification using the RF algorithm demonstrate the effectiveness of this method, especially in identifying mangroves in low-density areas. Specifically, the RF algorithm demonstrated strong performance in regions with sparse mangrove coverage, such as Charak Port and Tang Port. This indicates the algorithm’s high sensitivity to subtle variations in satellite imagery and its ability to accurately differentiate features. By capturing more complex features, such as spectral diversity and small-scale surface variations, the algorithm effectively identified mangrove forests in areas with low vegetation density. In contrast, in regions with higher mangrove density, such as Dargahan and Sirik, the RF algorithm maintained high accuracy, demonstrating its stability and effectiveness in different settings. These results are consistent with studies by Ghorbanian *et al*. (2021), Behera *et al*. (2021), and Purwanto *et al*. (2022), which also highlighted the effectiveness of this algorithm in mangrove forest identification.

The results indicate that remote sensing products face significant challenges in accurately identifying mangrove forests. While products like ESA and GLC produced acceptable results in some areas, their performance was poor in others, particularly in Mahshahr Port and Tang Port. These findings suggest that remote sensing products, especially in regions with lower density and more complex conditions, struggle to accurately detect mangrove forests. Specifically, the ESA product failed to identify mangrove forests in certain key areas, with the mangrove class accuracy recorded as zero in these locations, highlighting its limitations in these regions. In contrast, GLC and GMW products performed better in other areas, successfully identifying extensive mangrove forest regions, particularly in Qeshm and Kolgan.

Consequently, these comparisons demonstrate that no single product performed consistently well across all areas; rather, each product exhibited better capabilities in specific regions.

The results of this study indicate that Sentinel-2-based methods, particularly the MVI index, achieved the highest accuracy in identifying the mangrove class (95%), while the RF classifier with Sentinel-2 data provided an accuracy of 91% for mangroves. Both methods reached 98% accuracy in certain sites, such as Dargahan, Sirik, and Qeshm. In comparison, Landsat-9-based methods showed lower accuracy (MVI: 84%, RF: 86%). Global products exhibited weaker performance; GLC mapped the largest area (15,814 ha) but had an accuracy of 80% for the mangrove class, while ESA and GMW achieved 83% and 78% accuracy, respectively. Some of these products failed to detect mangroves in several sites, such as Mahshahr Port, Tang Port, Chabahar Port, Charak Port, Dayyer Port, BandarAbbas, Nakhiloo National Park, Hormoz Island, Pozm Tiyab Bay, Deirstan Bay, Nayband Bay, Chakhah, Kolahi and Tiyab Inlet, Kulaghan, Gwatar, Gabrik, and Jask Protected Area. The choice of the optimal method depends on the study's objective—whether higher accuracy or broader coverage is prioritized.

The findings of this study, in line with those of Maurya *et al*. (2021), Lu *et al*. (2022), and Sunkur *et al*. (2024), highlight the significant role of remote sensing in mapping and assessing mangrove forests. The results show that remote sensing is an effective tool for accurately identifying mangrove cover, an essential aspect for monitoring the condition of these ecosystems. Mangrove forests, due to their ecological importance and unique geographic location, are highly vulnerable to human activities and climate change. The analysis of remote sensing data demonstrates its potential to support the detection and evaluation of mangrove areas, which is crucial for informed conservation and management efforts.

The findings of this study contribute significantly to the understanding of mangrove forest ecosystems and the importance of accurate remote sensing data in assessing their condition. These results can guide future research and helping to better understand mangrove distribution and dynamics. Strengthening collaborations at both local and international levels, especially with communities that depend on these ecosystems, along with increased investment in the protection and restoration of mangrove forests, is crucial for their preservation. Additionally, raising public awareness about the economic and environmental significance of mangrove forests will enhance conservation efforts. However, the limitations of using satellite data and classification algorithms, particularly in areas with rapid environmental changes, should be acknowledged. Future studies could benefit from higher resolution data and an expanded geographical scope to provide deeper insights into natural resource management and conservation strategies.

5. Conclusion

The results of this study show that the use of multi-source data combined with advanced machine learning algorithms has played a significant role in the identification of mangrove forests. Through the comparison of the performance of various sensors, such as Sentinel-2 and Landsat-9, this research demonstrated that Sentinel-2 images offer higher accuracy in detecting mangrove forests, especially in areas with low vegetation density and high complexity. Furthermore, selecting an appropriate threshold in the classification process, particularly when using various indices, significantly improved accuracy and reduced detection errors. It is recommended not to use global products for evaluating mangrove forests in Iran, as these products are unable to fully identify mangrove areas in the country. Future studies should consider using radar data to improve the accuracy of vegetation classification. Combining radar data with optical and hyperspectral imagery can enhance the accuracy of mangrove mapping

and facilitate their differentiation from other vegetation types. Additionally, hyperspectral imagery, by providing more comprehensive information, can assist in more precise identification and biomass estimation. One of the challenges in Iran is the lack of ground truth data for training samples. Providing such data would not only save researchers' time but also enable diverse studies on various products across a wide spatial range (at the national level).

Author contributions

Mohammadreza Miandej performed the analysis and wrote the original draft. Qadir Ashournejad designed the study, supervised the work, and reviewed the manuscript. Fateme Garshasbi conducted the final revisions and editing. All authors contributed to discussing the results and improving the manuscript.

Data Availability Statement

Not applicable

Acknowledgment

We thank the editor, associate editor and reviewers for all their suggestions for improving the paper.

Funding

This research did not receive any specific grant from funding agencies in the public, commercial, or not-for-profit sectors.

Conflict of interest

The authors declare no conflict of interest. The funders had no role in the design of the study; in the collection, analyses, or interpretation of data; in the writing of the manuscript, or in the decision to publish the results.

Reference

Ambarwari, A., & Husni, E. M. (2023). Studying How Machine Learning Maps Mangroves in Moderate-Resolution Satellite Images. *Indonesian Journal of Artificial Intelligence and Data Mining*, 6(2), 270-280. http://dx.doi.org/10.24014/ijaidm.v6i2.25263

Ashournejad, Q., Amiraslani, F., Kiyavarz Moghaddam, M., & Tomanian, A. (2019a). Impacts of Landuse/Landcover Changes on the Ecosystem Service Values in Pars Special Economic Energy Zone Using Remote Sensing. *Physical Geography Research*, 51(2), 317-333. https://doi.org/10.22059/jphgr.2019.270215.1007303

Ashournejad, Q., Amiraslani, F., Kiavarz Moghadam, M., Toomanian, A., (2019b). Assessing the changes of mangrove ecosystem services value in the Pars Special Economic Energy Zone. *Ocean & Coastal Management* 179, 104838. https://doi.org/10.1016/j.ocecoaman.2019.104838

Ashournejad, Q. (2022). Economic evaluation of tourism ecosystem services of Iran's biomes based on remote sensing products. *Journal of Tourism Planning and Development*, *10*(39), 141-162. https://doi.org/10.22080/jtpd.2022.22179.3603

Ashournejad, Q. (2023). Evaluation and comparison of regional accuracy of global remote sensing products in Iran-Case study of land cover products in Mazandaran Province. *Scientific-Research Quarterly of Geographical Data (SEPEHR)*, *32*(127), 95-115. https://doi.org/10.22131/sepehr.2023.1988986.2954

Baloloy, A. B., Blanco, A. C., Ana, R. R. C. S., & Nadaoka, K. (2020). Development and application of a new mangrove vegetation index (MVI) for rapid and accurate mangrove mapping. *ISPRS Journal of Photogrammetry and Remote Sensing*, 166, 95-117. https://doi.org/10.1016/j.isprsjprs.2020.06.001

Behera, M. D., Barnwal, S., Paramanik, S., Das, P., Bhattyacharya, B. K., Jagadish, B., ... & Behera, S. K. (2021). Species-level classification and mapping of a mangrove forest using random forest—utilisation of AVIRIS-NG and sentinel data. *Remote Sensing*, *13*(11), 2027. https://doi.org/10.3390/rs13112027

Bihamta Toosi, N., Soffianian, A. R., Fakheran, S., Pourmanafi, S., Ginzler, C., & T. Waser, L. (2020). Land cover classification in mangrove ecosystems based on VHR satellite data and machine learning—an upscaling approach. *Remote Sensing*, *12*(17), 2684. https://doi.org/10.3390/rs12172684

Bie, Q., Shi, Y., Li, X., & Wang, Y. (2022). Contrastive analysis and accuracy assessment of three global 30 m land cover maps circa 2020 in arid land. *Sustainability*, 15(1), 741. https://doi.org/10.3390/su15010741

Bunting, P., Rosenqvist, A., Hilarides, L., Lucas, R. M., Thomas, N., Tadono, T., ... & Rebelo, L. M. (2022). Global mangrove extent change 1996–2020: Global mangrove watch version 3.0. *Remote Sensing*, *14*(15), 3657. https://doi.org/10.3390/rs14153657

Chaaban, F., El Khattabi, J., & Darwishe, H. (2022). Accuracy assessment of ESA WorldCover 2020 and ESRI 2020 land cover maps for a Region in Syria. *Journal of Geovisualization and Spatial Analysis*, 6(2), 31. https://doi.org/10.1007/s41651-022-00126-w

Congalton, R. G. (1991). A review of assessing the accuracy of classifications of remotely sensed data. *Remote sensing of environment*, *37*(1), 35-46. https://doi.org/10.1016/0034-4257(91)90048-B

Conopio, M., Baloloy, A. B., Medina, J., & Blanco, A. C. (2021). Spatio-temporal mapping and analysis of mangrove extents around Manila Bay using Landsat satellite imagery and Mangrove Vegetation Index (MVI). *The International Archives of the Photogrammetry, Remote Sensing and Spatial Information Sciences*, *46*, 103-108. https://doi.org/10.5194/isprs-archives-XLVI-4-W6-2021-103-2021

de Araujo Barbosa, C. C., Atkinson, P. M., & Dearing, J. A. (2015). Remote sensing of ecosystem services: A systematic review. *Ecological Indicators*, 52, 430-443. https://doi.org/10.1016/j.ecolind.2015.01.007

Elmahdy, S. I., Ali, T. A., Mohamed, M. M., Howari, F. M., Abouleish, M., & Simonet, D. (2020). Spatiotemporal mapping and monitoring of mangrove forests changes from 1990 to 2019 in the Northern Emirates, UAE using random forest, Kernel logistic regression and Naive Bayes Tree models. *Frontiers in Environmental Science*, 8, 102. https://doi.org/10.3389/fenvs.2020.00102

Erfanifard, Y., Lotfi Nasirabad, M., & Stereńczak, K. (2022). Assessment of Iran's mangrove forest dynamics (1990–2020) using Landsat time series. *Remote Sensing*, 14(19), 4912. https://doi.org/10.3390/rs14194912

Erfanifard, Y., & Lotfi Nasirabad, M. (2022). Efficiency of Mangrove Indices in Mapping Some Mangrove Forests Using Landsat 8 Imagery in Southern Iran. *RS and GIS for Natural Resources*, 13(4), 68–86. https://doi.org/10.30495/girs.2022.685675

Erfanifard, Y., & Lotfi Nasirabad, M. (2023). Mapping mangrove forest extent in Iran using Sentinel-2 imagery. *Iranian Journal of Forest and Poplar Research*, 31(2), 98-112. https://doi.org/10.22092/IJFPR.2023.360820.2081

Fatemi, S.B., & Rezaei, Y. (Eds.). (2023). *Fundamentals of Remote Sensing*: 6th Edition. Azadeh Press.

Garshasbi, F., Ashournejad, Q., & Ghalenoei, N. (2025). A comparative assessment of remote sensing based land cover products for economic valuation of ecosystem services of Hyrcanian forests. *Advances in Space Research*. https://doi.org/10.1016/j.asr.2024.12.064

Gholami, D. M., & Baharlouii, M. (2019). Monitoring long-term mangrove shoreline changes along the northern coasts of the Persian Gulf and the Oman Sea. *Emerging Science Journal*, 3(2), 88-100. https://doi.org/10.28991/esj-2019-01172

Ghorbanian, A., Zaghian, S., Asiyabi, R. M., Amani, M., Mohammadzadeh, A., & Jamali, S. (2021). Mangrove ecosystem mapping using Sentinel-1 and Sentinel-2 satellite images and random forest algorithm in Google Earth Engine. *Remote sensing*, 13(13), 2565. https://doi.org/10.3390/rs13132565

Grekousis, G., Mountrakis, G., & Kavouras, M. (2015). An overview of 21 global and 43 regional land-cover mapping products. *International Journal of Remote Sensing*, 36(21), 5309-5335. https://doi.org/10.1080/01431161.2015.1093195

Gupta, K., Mukhopadhyay, A., Giri, S., Chanda, A., Majumdar, S. D., Samanta, S., ... & Hazra, S. (2018). An index for discrimination of mangroves from non-mangroves using LANDSAT 8 OLI imagery. *MethodsX*, 5, 1129-1139. https://doi.org/10.1016/j.mex.2018.09.011

Ibharim, N. A., Mustapha, M. A., Lihan, T., & Mazlan, A. G. (2015). Mapping mangrove changes in the Matang Mangrove Forest using multi temporal satellite imageries. *Ocean & coastal management*, *114*, 64-76. https://doi.org/10.1016/j.ocecoaman.2015.06.005

Jia, M., Wang, Z., Mao, D., Ren, C., Song, K., Zhao, C., ... & Wang, Y. (2023). Mapping global distribution of mangrove forests at 10-m resolution. *Science Bulletin*, 68(12), 1306-1316. https://doi.org/10.1016/j.scib.2023.05.004

Khan, W. R., Nazre, M., Akram, S., Anees, S. A., Mehmood, K., Ibrahim, F. H., ... & Zhu, X. (2024). Assessing the productivity of the Matang Mangrove Forest reserve: Review of one of the best-managed mangrove forests. *Forests*, *15*(5), 747. https://doi.org/10.3390/f15050747

Kiyani, V., Alizade Shaabani, A., & Nazari Samani, A. (2014). Assessing the Classification accuracy of LISS-III Sensor Image of IRS-P6 Satellite using Google Earth'sDatabase to provide land coverage/ Land use maps (Case study: Taleghan Watershed). *Quarterly of Geographical Data*, 23(90), 51-59. https://doi.org/10.22131/sepehr.2014.12167

Li, L., Wang, Y., & Liu, C. (2014). Effects of land use changes on soil erosion in a fast developing area. *International Journal of Environmental Science and Technology*, 11, 1549-1562. https://doi.org/10.1007/s13762-013-0341-x

Lillesand, T., Kiefer, R. W., & Chipman, J. (2015). *Remote sensing and image interpretation*. John Wiley & Sons.

Liu, J., Ren, Y., & Chen, X. (2023). Regional Accuracy Assessment of 30-Meter GLC_FCS30, GlobeLand30, and CLCD Products: A Case Study in Xinjiang Area. *Remote Sensing*, 16(1), 82. https://doi.org/10.3390/rs16010082

Lu, Y., & Wang, L. (2021). How to automate timely large-scale mangrove mapping with remote sensing. *Remote Sensing of Environment*, *264*, 112584. https://doi.org/10.1016/j.rse.2021.112584

Lu, Y., & Wang, L. (2022). The current status, potential and challenges of remote sensing for large-scale mangrove studies. *International Journal of Remote Sensing*, 43(18), 6824-6855. https://doi.org/10.1080/01431161.2022.2145584

Maurya, K., Mahajan, S., & Chaube, N. (2021). Remote sensing techniques: Mapping and monitoring of mangrove ecosystem—A review. *Complex & Intelligent Systems*, *7*(6), 2797-2818. https://doi.org/10.1007/s40747-021-00457-z

Miraki, M., Sohrabi, H., Sadeghi, S., Fatehi, P., & Immitzer, M. (2023). Application of mangrove recognition index for mapping mangrove forests using Sentinel-2 satellite images in Google Earth Engine. *Journal of Marine Science and Technology*, 22(3), 40-49. https://doi.org/10.22113/jmst.2022.318177.2456

Naderloo, R., Shahdadi, A., Rahymanian, H., Ghodrati Shojaei, M., & Nasrollahi, A. (2024). *Atlas of Sensitive Marine Ecosystems of Iran (Persian Gulf and Oman Sea)*. Tehran University Press

Neri, M. P., Baloloy, A. B., & Blanco, A. C. (2021). Limitation assessment and workflow refinement of the Mangrove Vegetation Index (MVI)-based mapping methodology using Sentinel-2 imagery. *The International Archives of the Photogrammetry, Remote Sensing and Spatial Information Sciences*, 46, 235-242. https://doi.org/10.5194/isprs-archives-XLVI-4-W6-2021-235-2021

Purwanto, A. D., Wikantika, K., Deliar, A., & Darmawan, S. (2022). Decision tree and random forest classification algorithms for mangrove forest mapping in Sembilang National Park, Indonesia. *Remote Sensing*, 15(1), 16. https://doi.org/10.3390/rs15010016

Rahman, M. M., Zhang, X., Ahmed, I., Iqbal, Z., Zeraatpisheh, M., Kanzaki, M., & Xu, M. (2020). Remote sensing-based mapping of senescent leaf C: N ratio in the sundarbans reserved forest using machine learning techniques. *Remote Sensing*, 12(9), 1375. https://doi.org/10.3390/rs12091375

Raza, S. A., Zhang, L., Zuo, J., & Chen, B. (2024). Time series monitoring and analysis of Pakistan's mangrove using Sentinel-2 data. *Frontiers in Environmental Science*, 12, 1416450. https://doi.org/10.3389/fenvs.2024.1416450

Sahraei, R., Ghorbanian, A., Kanani-Sadat, Y., Jamali, S., & Homayouni, S. (2023). Identifying suitable locations for mangrove plantation using geospatial information system and remote sensing. *ISPRS Annals of the Photogrammetry, Remote Sensing and Spatial Information Sciences*, 10, 669-675. https://doi.org/10.5194/isprs-annals-X-4-W1-2022-669-2023

Safiari, S. (2017). Mangrove forests in Iran. *Iran nature*, 2(2), 49-57. https://doi.org/10.22092/irn.2017.111425

Shen, Z., Miao, J., Wang, J., Zhao, D., Tang, A., & Zhen, J. (2023). Evaluating Feature Selection Methods and Machine Learning Algorithms for Mapping Mangrove Forests Using Optical and Synthetic Aperture Radar Data. *Remote Sensing*, 15(23), 5621. https://doi.org/10.3390/rs15235621

Sobhani, P., & Danehkar, A. (2023). Evaluating and zoning of ecosystem services in mangrove forests of Khamir and Qeshm. *Town and Country Planning*, 15(2), 275-292. https://doi.org/10.22059/jtcp.2023.358990.670391

Sunkur, R., Kantamaneni, K., Bokhoree, C., Rathnayake, U., & Fernando, M. (2024). Mangrove mapping and monitoring using remote sensing techniques towards climate change resilience. *Scientific Reports*, 14(1), 6949. https://doi.org/10.1038/s41598-024-57563-4

Tran, T. V., Reef, R., & Zhu, X. (2022). A review of spectral indices for mangrove remote sensing. *Remote Sensing*, 14(19), 4868. https://doi.org/10.3390/rs14194868

Tso, B., & Mather, P. M. (2003). *Classification methods for remotely sensed data*. CRC Press.

Toosi, N. B., Soffianian, A. R., Fakheran, S., Pourmanafi, S., Ginzler, C., & Waser, L. T. (2019). Comparing different classification algorithms for monitoring mangrove cover changes in southern Iran. *Global Ecology and Conservation*, 19, e00662. https://doi.org/10.1016/j.gecco.2019.e00662

Valero-Jorge, A., González-Lozano, R., Zayas, G. D., Matos-Pupo, F., Sorí, R., & Stojanovic, M. (2024). An Innovative Tool for Monitoring Mangrove Forest Dynamics in Cuba Using Remote Sensing and WebGIS Technologies: SIGMEM. *Remote Sensing* . https://doi.org/10.3390/rs16203802

Wang, D., Wan, B., Qiu, P., Su, Y., Guo, Q., Wang, R., ... & Wu, X. (2018). Evaluating the performance of Sentinel-2, Landsat 8 and Pléiades-1 in mapping mangrove extent and species. *Remote Sensing*, 10(9), 1468. https://doi.org/10.3390/rs10091468

Wu, X., Xiao, Q., Wen, J., You, D., & Hueni, A. (2019). Advances in quantitative remote sensing product validation: Overview and current status. *Earth-Science*, 196, 102875. https://doi.org/10.1016/j.earscirev.2019.102875

Xiao, Z., Jiang, W., Wu, Z., Ling, Z., Deng, Y., Zhang, Z., & Peng, K. (2024). Agreement Analysis and Accuracy Assessment of Multiple Mangrove Datasets in Guangxi Beibu Gulf and Guangdong-Hong Kong-Macau Greater Bay, China, for 2000-2020. *IEEE Journal of Selected Topics in Applied Earth Observations and Remote Sensing*. https://doi.org/10.1109/JSTARS.2024.3353251

Yang, G., Huang, K., Sun, W., Meng, X., Mao, D., & Ge, Y. (2022). Enhanced mangrove vegetation index based on hyperspectral images for mapping mangrove. *ISPRS Journal of Photogrammetry and Remote Sensing*, *189*, 236-254. https://doi.org/10.1016/j.isprsjprs.2022.05.003

Zanaga, D., Van De Kerchove, R., De Keersmaecker, W., Souverijns, N., Brockmann, C., Quast, R., Wevers, J., Grosu, A., Paccini, A., Vergnaud, S., Cartus, O., Santoro, M., Fritz, S., Georgieva, I., Lesiv, M., Carter, S., Herold, M., Li, Linlin, Tsendbazar, N.E., Ramoino, F., Arino, O., (2021). ESA WorldCover 10 m 2020 v100. https://doi:10.5281/zenodo.5571936

Zanganeh Asadi, M.A., TaghaviMoghadam, E., & Akbari, E.(2017). Evaluation and assessment of changes in forest area Harra (mangrove) Using remote sensing techniques Case Study: Bandar Abbas, *Natural Ecosystems of Iran*, 7(4),17-32. https://sanad.iau.ir/en/Article/983173?FullText=FullText

Zhang, X., Zhao, T., Xu, H., Liu, W., Wang, J., Chen, X., & Liu, L. (2024). GLC_FCS30D: the first global 30 m land-cover dynamics monitoring product with a fine classification system for the period from 1985 to 2022 generated using dense-time-series Landsat imagery and the continuous change-detection method. *Earth System Science Data*, 16(3), 1353-1381. https://doi.org/10.5194/essd-16-1353-2024

Zanvo, M. S., Barima, Y. S., Salako, K. V., Koua, K. N., Kolawole, M. A., Assogbadjo, A. E., & Kakaï, R. G. (2021). Mapping spatio-temporal changes in mangroves cover and projection in 2050 of their future state in Benin. *BOIS & FORETS DES TROPIQUES*, 350, 29-42. https://doi.org/10.19182/bft2021.350.a36828